Planet Detection Metrics:

Robovetter Completeness and Effectiveness for Data Release 25

KSCI-19114-001

Jeffrey L. Coughlin

May 25, 2017

Prepared by: _____ Date: ___5/25/17___
Jeffrey L. Coughlin, *Kepler* Science Office

Approved by: _____ Date: ___5/25/17___
Natalie Batalha, *Kepler* Project Scientist

Approved by: _____ Date: ___5/25/17___
Michael R. Haas, *Kepler* Science Office Director

Document Control

Ownership
This document is part of the Kepler Project Documentation that is controlled by the Kepler Project Office, NASA/Ames Research Center, Moffett Field, California.

Control Level
This document will be controlled under KPO @ Ames Configuration Management system. Changes to this document shall be controlled.

Physical Location
The physical location of this document will be in the KPO @ Ames Data Center.

Distribution Requests
To be placed on the distribution list for additional revisions of this document, please address your request to the Kepler Science Office:

> Michael R. Haas
> Kepler Science Office Director
> MS 244-30
> NASA Ames Research Center
> Moffett Field, CA 94035-1000
> Michael.R.Haas@nasa.gov

The correct citation for this document is: J.L. Coughlin 2017, *Planet Detection Metrics: Robovetter Completeness and Effectiveness for Data Release 25*, KSCI-19114-001

DOCUMENT CHANGE LOG

CHANGE DATE	PAGES AFFECTED	CHANGES/NOTES
May 25, 2017		Original release

Contents

1   Introduction

In general, the *Kepler* pipeline identifies a list of Threshold Crossing Events (TCEs), which are periodic flux decrements meeting certain criteria (Jenkins, 2017). These TCEs are reviewed and those that appear consistent with astrophysically transiting or eclipsing systems are classified as Kepler Objects of Interest (KOIs). Further review is given to KOIs, which are then dispositioned as Planet Candidates (PCs) or False Positive (FPs). FPs are further denoted by four major flags that indicate if the signal is Not Transit-Like (NTL), due to a Stellar Eclipse (SS; previously referred to as "Significant Secondary"), and/or due to contamination from a source other than the target as evidenced by a Centroid Offset (CO) or an Ephemeris Match (EM) with another object. This entire TCE review process is known as "dispositioning" or "vetting".

In the first five *Kepler* mission planet candidate catalogs (Borucki et al., 2011a,b; Batalha et al., 2013; Burke et al., 2014; Rowe et al., 2015), TCEs were manually examined on an individual basis and dispositioned using various plots and quantitative diagnostic tests (see e.g., Coughlin, 2017). In the sixth catalog, Mullally et al. (2015a) employed partial automation via simple parameter cuts to automatically disposition a large fraction of TCEs as not transit-like. Mullally et al. (2015a) also used an automated technique known as the "centroid Robovetter" (Mullally, 2017) to automatically identify some FP KOIs due to centroid offsets — a telltale signature of light contamination from another target. The remaining targets were manually dispositioned. In the seventh catalog, Coughlin et al. (2016) automated the entire dispositioning process using what is collectively known simply as "the Robovetter". In the eighth and final mission catalog, Thompson et al. (2017) use a revised Robovetter to automate the dispositioning of all TCEs with an emphasis on creating a catalog suitable for accurately determining planet occurrence rates.

In order to calculate accurate occurrence rates, the completeness and effectiveness of the Robovetter must be characterized. We define these terms as applied to the Robovetter, following Thompson et al. (2017), as:

- Completeness — The fraction of transiting planets detected by the pipeline that are classified as planet candidates by the Robovetter.

- Effectiveness — The fraction of false positives detected by the pipeline that are classified as false positives by the Robovetter.

The remainder of this document describes products that can be used to quantitatively assess Robovetter completeness and effectiveness for an arbitrary set of *Kepler* stars. The completeness of the *Kepler* pipeline is addressed separately (see Christiansen, 2017; Burke & Catanzarite, 2017a,b), and we stress that both are required for the calculation of accurate occurrence rates. Christiansen (2017) characterizes the completeness of the *Kepler* pipeline by injecting artificial transits in the pixel-level data, re-running the *Kepler* pipeline, and measuring the number of injected TCEs (injTCEs) that are recovered. Burke & Catanzarite (2017a) utilize the results and those from flux-level transit injection (Burke & Catanzarite, 2017b) to construct per target detection contours, which account for pipeline completeness.

Since the population of TCEs from the *Kepler* pipeline are dominated by false positives (Thompson et al., 2017), an accurate measure of Robovetter effectiveness is required to

accurately determine the fraction of planet candidates that are actually transiting planets (i.e., the "Reliability" of the sample). As part of characterizing effectiveness, some transit signals were injected purposely off-target to simulate centroid-offset false positives, and some transit signals were injected with secondary eclipses to simulate eclipsing-binary (EB) false positives (Christiansen, 2017). Two separate activities were also conducted to simulate false positives due to variable stars and instrumental artifacts. In the first, the *Kepler* pipeline was re-run with the light curves inverted immediately before the planet search to produce inverted TCEs (invTCEs). In the second, the light curves were scrambled by re-arranging the data in per-quarter or per-month chunks immediately before the planet search to produce scrambled TCEs (scrTCEs). Since inversion and scrambling should eliminate all legitimate transits, but preserve the general noise properties of the flux time series, these invTCEs and scrTCEs should be almost exclusively FPs.

This document describes the results of running the Robovetter on the observed, injected, inverted, and scrambled populations, which are available at the NASA Exoplanet Archive[1]. In §2 we describe the experimental design to calculate the Robovetter completeness and effectiveness. In §3 we describe the tables that contain the results of running the Robovetter on the obs, inj, inv, and scrTCEs. Finally, in §4 we show some example results that can be used to compute accurate occurrence rates. In an accompanying document, Coughlin (2017) describes the DR25 TCERT vetting forms used to assess Robovetter performance; they are available at NExScI for every obs, inj, inv, and scrTCE described herein.

2 Experimental Design

In the following subsections we describe each dataset and their relevance to measuring the Robovetter's completeness and effectiveness. Note that the Robovetter code is publicly available[2], along with input files for each dataset that contain all metrics used by the Robovetter, and output files that provide the resulting dispositions, scores, and major/minor flags.

2.1 Observed

As described in Twicken et al. (2016), the *Kepler* pipeline was used to search the 198,640 observed (obs) light curves from Q1–Q17 Data Release 25 (DR25), resulting in the detection of 32,534 obsTCEs. Note that this number, and all TCE counts stated in this document, do not include 'rogue' TCEs, which were discovered after the obsTCE table was created and Twicken et al. (2016) was published. A column entitled "Rogue Flag" has been added to the DR25 TCE table at NExScI to flag these rogue TCEs (i.e., tce_rogue_flag).

Rogue TCEs are signals that should have failed the "three-transit weight check" (see Section 2 of Burke & Catanzarite, 2017c) in the transiting planet search (TPS) module of the *Kepler* pipeline, but were inadvertently made into TCEs due to an error in the code. There were 1,498 rogue TCEs among the original set of 34,032 obsTCEs. Because these rogue TCEs are not modeled by the occurrence rate products which characterize the TPS module, they should not be included in occurrence rate calculations using these products.

---

[1]`exoplanetarchive.ipac.caltech.edu`

[2]`https://github.com/nasa/kepler-robovetter`

Consequently, only the 32,534 obsTCEs were vetted by the Robovetter to produce the KOIs found in the DR25 KOI catalog (Thompson et al., 2017).

2.2   Injection

As described in Christiansen (2017), the signatures of simulated transiting planets were injected into the DR25 calibrated pixels of 198,640 target stars across the focal plane. The pixel-level data was then processed through the DR25 version of the *Kepler* pipeline, including light curve creation and detrending, transiting planet search, and data validation. In total, there were 74,776 injTCEs recovered by the pipeline with a similar enough period and epoch compared to the injected period and epoch (Christiansen, 2017). Note that while many of the observed TCEs are found when searching the injected data, the injTCEs only include TCEs that are a result of an injection.

The injections fall into three categories:

1. 45,377 injTCEs are due to injections of single planets at the nominal positions of their target stars.

2. 18,897 injTCEs are due to injections of single planets positionally off-target (i.e., they were injected with a centroid offset).

3. 10,502 injTCEs are due to injections of two on-target planets on each star with the same period, but different epochs, to simulate a population of EBs.

In the data tables provided by Christiansen (2017), Group #1 is indicated by values of 0 for both "Offset_from_source" and "EB_injection". Group #2 is indicated by a value of 1 for "Offset_from_source" and a value of 0 for "EB_injection". Group #3 is indicated by a value of 1 for "EB_injection".

The set of successfully recovered on-target single planet injTCEs (Group #1) can be used to determine the Robovetter completeness. Specifically, it can answer:

- How often does the Robovetter classify an injected planet as a planet candidate?

- Does the Robovetter completeness significantly vary with signal-to-noise ratio, period, or other parameters?

- Which Robovetter tests/modules most often fail injected planets, and for what reasons?

The set of off-target single planet injTCEs (Group #2) can be used to help characterize the Robovetter effectiveness. Specifically, how often does the Robovetter correctly identify off-target signals, and how does this vary as a function of the offset, stellar, and planet parameters? Similarly, the set of on-target EB TCEs (Group #3) can be used to determine how effective the Robovetter is at detecting secondary eclipses that are indicative of EBs, and how this varies as a function of the primary transit, secondary eclipse, and stellar parameters.

2.3   Inversion

A new experiment was introduced in DR25 called "light curve inversion". The *Kepler* pipeline was modified to run on the exact same light curves that were searched for planets in the observed run with the added step of inverting the light curves immediately before the planet search. Specifically, after each light curve was detrended and normalized to a baseline flux of 0.0, it was multiplied by -1.0 to invert the light curve. This resulted in 19,536 invTCEs, which were then dispositioned with the same version of the Robovetter as the obsTCEs. Since planetary transits only result in a decrease of flux, and any invTCEs are due to an increase of flux in the observed light curves, the invTCEs represent a set of not transit-like TCEs, which can be used to help determine the Robovetter's effectiveness. Specifically, how often does the Robovetter correctly identify quasi-sinusoidal, not transit-like signals? Note that while many of *Kepler's* not transit-like false positives are due to quasi-sinusoidal signals that are symmetrical under inversion, some are not (e.g., Sudden Pixel Sensitivity Dropouts [SPSDs; Van Cleve et al., 2016]). Thus, another method of generating false positives is needed to cover all NTL cases (see §2.4).

2.4   Scrambling

Another new experiment introduced in DR25 is called "light curve scrambling". In this case, the *Kepler* pipeline was modified to run on the exact same light curves that were searched for planets in the observed run with the added step of scrambling the light curves immediately before the planet search. Specifically, after each light curve was normalized, the timestamps on selected blocks of cadences were swapped according to the specified scrambling order. Multiple runs were conducted with different scrambling orders, each one keeping whole quarters of observations together in order to preserve noise and systematics that occur on those timescales. For example, a large number of false positive TCEs are produced by the quarterly roll of the spacecraft, which results in some targets falling on a CCD with increased systematic noise every fourth quarter (i.e., seasonally). While the nominal, observed order is Q1, Q2, Q3...Q16, Q17, the scrambled light curve runs were done with the following orderings:

1. Q13, Q14, Q15, Q16, Q9, Q10, Q11, Q12, Q5, Q6, Q7, Q8, Q1, Q2, Q3, Q4, Q17

2. Q1, Q2, Q3, Q4, Q13, Q14, Q15, Q16, Q9, Q10, Q11, Q12, Q5, Q6, Q7, Q8, Q17

3. Q16, Q15, Q14, Q13, Q12, Q11, Q10, Q9, Q8, Q7, Q6, Q5, Q4, Q3, Q2, Q1, Q17

At the time of this writing, scrTCEs from ordering #1 have been dispositioned with the same version of the Robovetter as the obsTCEs. However, the Robovetter has not yet been run on orderings #2 and #3.

As planet transits are linearly periodic events (or very nearly linearly periodic in the few cases of systems with significant TTVs), the scrTCEs represent a set of not transit-like TCEs. Compared to the invTCEs, scrTCEs better represent not transit-like false positives due to SPSDs and other non-invertible phenomenon, though less well represent not transit-like false positives associated with the ∼372 day rolling-band artifacts and other coherent quasi-sinusoidal phenomena.

3   Robovetter Disposition Tables

We present the parameters that are needed to compute the completeness and effectiveness of the Robovetter in the Robovetter Disposition Tables, which are hosted at the NASA Exoplanet Archive. These tables contain information on every obsTCE, injTCE, invTCE, and scrTCE. The tables are in IPAC ASCII format[3], and the headers contains information on the IPAC format and links to Python[4] and IDL[5] modules to read them. Each file contains 25 columns, which include the Robovetter dispositions and major Robovetter vetting flags, and the planetary parameters from the Data Validation (DV) module of the *Kepler* pipeline. Note that there was a bug in the DR25 DV module that caused the best-fit search to always assume a large initial value for the impact parameter, which resulted in final planetary fits with a significant bias towards high impact parameters and large planetary radii (Christiansen, 2017). After the public release of the DR25 obsTCEs and the publication of Twicken et al. (2016), this bug was fixed so that the initial seeds had more uniform impact parameters, and the DV fits were re-computed for all datasets. The parameters from these "supplemental" fits are shown in the Robovetter Disposition Tables — in a small percentage of cases a supplemental fit was not able to be computed, so the original DV parameters are shown instead. In order, the 25 columns in each table are:

1. TCE_ID — A unique identifier for each TCE from a pipeline run that consists of the target's *Kepler* Input Catalog (KIC) ID number, a dash, and then the planet number.

2. KIC — The KIC ID of the TCE.

3. Disp — The disposition of the TCE according to the DR25 version of the Robovetter. PC indicates it was dispositioned as a planet candidate, while FP indicates it was dispositioned as a false positive.

4. Score — The disposition score, which indicates the Robovetter's confidence in the given disposition. The score has a value between 0 and 1. Values close to one indicate high confidence in the disposition of a TCE as a PC. Values close to zero indicate high confidence in the disposition of a TCE as a FP.

5. NTL — A binary flag that indicates if the TCE was dispositioned as Not Transit-Like (NTL) by the Robovetter. A value of "1" indicates it was dispositioned as NTL.

6. SS — A binary flag that indicates if the TCE was dispositioned as having a Stellar Eclipse (SS) by the Robovetter. A value of "1" indicates it was dispositioned as SS.

7. CO — A binary flag that indicates if the TCE was dispositioned as having a Centroid Offset (CO) by the Robovetter. A value of "1" indicates it was dispositioned as CO.

8. EM — A binary flag that indicates if the TCE was dispositioned as having an Ephemeris Match (EM) by the Robovetter. A value of "1" indicates it was dispositioned as EM.

9. period — The period of the TCE in days as determined by the DV module.

---

[3]http://exoplanetarchive.ipac.caltech.edu/docs/ddgen/ipac_tbl.html
[4]http://docs.astropy.org/en/stable/api/astropy.io.ascii.Ipac.html
[5]https://irsa.ipac.caltech.edu/tools/pro/read_ipac_table.pro

10. epoch — The epoch of the TCE in Barycentric Kepler Julian Date (BKJD; Thompson et al., 2016) as determined by the DV module.

11. Expected_MES — The expected value for the Multiple Event Statistic (MES) based on the injection parameters. (Note this value is only known for the injected TCEs, and is set to "null" for the observed, inverted, and scrambled TCEs.)

12. MES — The Multiple Event Statistic (Jenkins, 2017) of the TCE, which is the *Kepler* pipeline's detection statistic, somewhat analogous to SNR. In the figures, the MES is also referred to as "Detected MES" in order to distinguish it from Expected MES.

13. NTran — The number of transits that were included when calculating the MES.

14. depth — The depth of the TCE in parts per million as determined by the DV module.

15. duration — The duration of the TCE in hours as determined by the DV module.

16. Rp — The radius of the planet in Earth radii as determined by the DV module.

17. Rs — The radius of the star in solar radii as used by the DV module.

18. Ts — The temperature of the star in Kelvin as used by the DV module.

19. logg — The surface gravity of the star in cm^2/s as used by the DV module.

20. a — The fitted semi-major axis of the orbit in AU as determined by the DV module.

21. Rp/Rs — The fitted radius ratio as determined by the DV module.

22. a/Rs — The fitted orbital scale as determined by the DV module.

23. SNR_DV — The SNR of the transit-model fit as determined by the DV module.

24. Sp — The inferred insolation flux in Earth units as determined by the DV module.

25. Fit_Prov — A flag indicating if the DV fit parameters come from supplemental fits (1) or original fits (0).

4   Example Results

In this section, using data from the provided tables, we show plots of the PC fraction (i.e., the fraction of TCEs dispositioned as PC) for the different TCE sets as a combination of various parameters. Using the major disposition flags in the tables, we also show plots that explore the fraction of TCEs dispositioned as transit-like (NTL=0), non-stellar eclipse (SS=0), and on-target (CO=0). These plots are meant to serve as examples of the types of analysis that can be conducted with these data sets.

In Figure 1 we show the PC fraction of the 32,534 obsTCEs, which contain a mix of real planets and all types of false positives. The vast majority (∼88%) of obsTCEs are dispositioned as FP, with very few PCs originating from long-period, low-MES obsTCEs. With respect to stellar parameters, it appears most FPs originate from non-main sequence, non-FGK stars, which may be due to increased stellar variability compared to main-sequence FGK stars (see bottom-left panel).
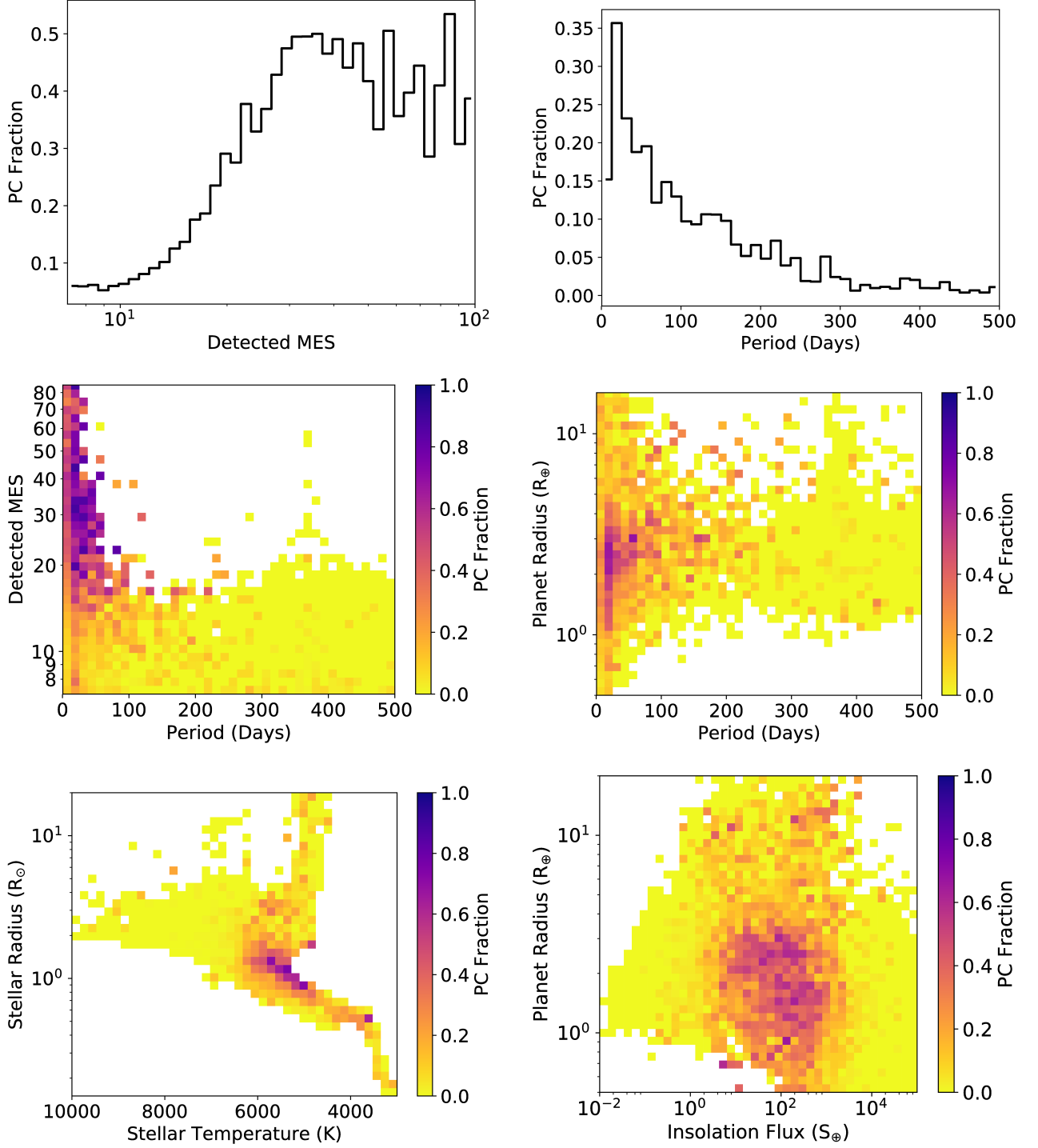
Figure 1: Examples of the PC fraction in the obsTCE population for different combinations of parameters. Top-left: The PC fraction as a function of the detected MES. Top-right: The PC fraction as a function of period. Middle-left: The PC fraction as a function of period and MES. Middle-right: The PC fraction as a function of period and the planet's radius. Bottom-left: The PC fraction as a function of the stellar radius and temperature. Bottom-right: The PC fraction as a function of the planet's radius and insolation flux. Note that bins/boxes with less than 5 TCEs are not displayed.

In Figure 2 we show the PC fraction of the 45,377 injTCEs that comprise the on-target single injected planet group (Group #1 of the injections) for 5 different period ranges, as well as for all periods. These period ranges correspond to those chosen by Burke & Catanzarite (2017a). In general the PC fraction decreases at lower values of Expected MES, and for longer periods.
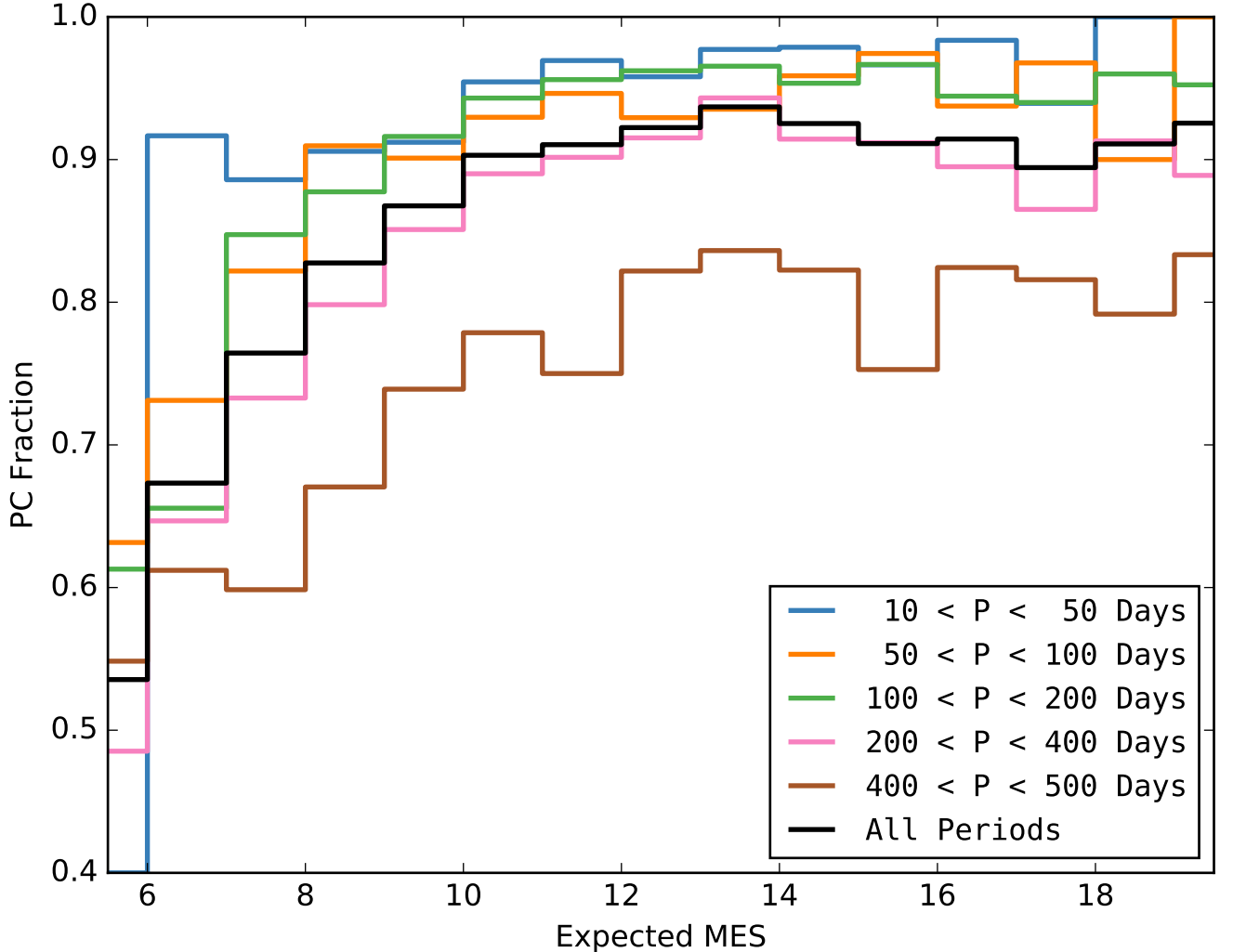

Figure 2: The PC fraction of the on-target single-injected planet population (Group 1) versus expected MES, for different period ranges.

In Figure 3 we show the PC fraction of the 45,377 injTCEs that comprise the on-target single injected planet group (Group #1 of the injections) for various combinations of parameters. If the Robovetter was perfect, all of these on-target injTCEs would be dispositioned as PC. In practice, ∼85% of on-target injections are dispositioned as PC. At high MES and short periods, the PC fraction is near 100%, but at the longest periods and lowest detected MES values it is ∼50%. The PC fraction is lower for evolved stars than main-sequence stars, likely as a result of the higher levels of photometric variation on transit timescales.
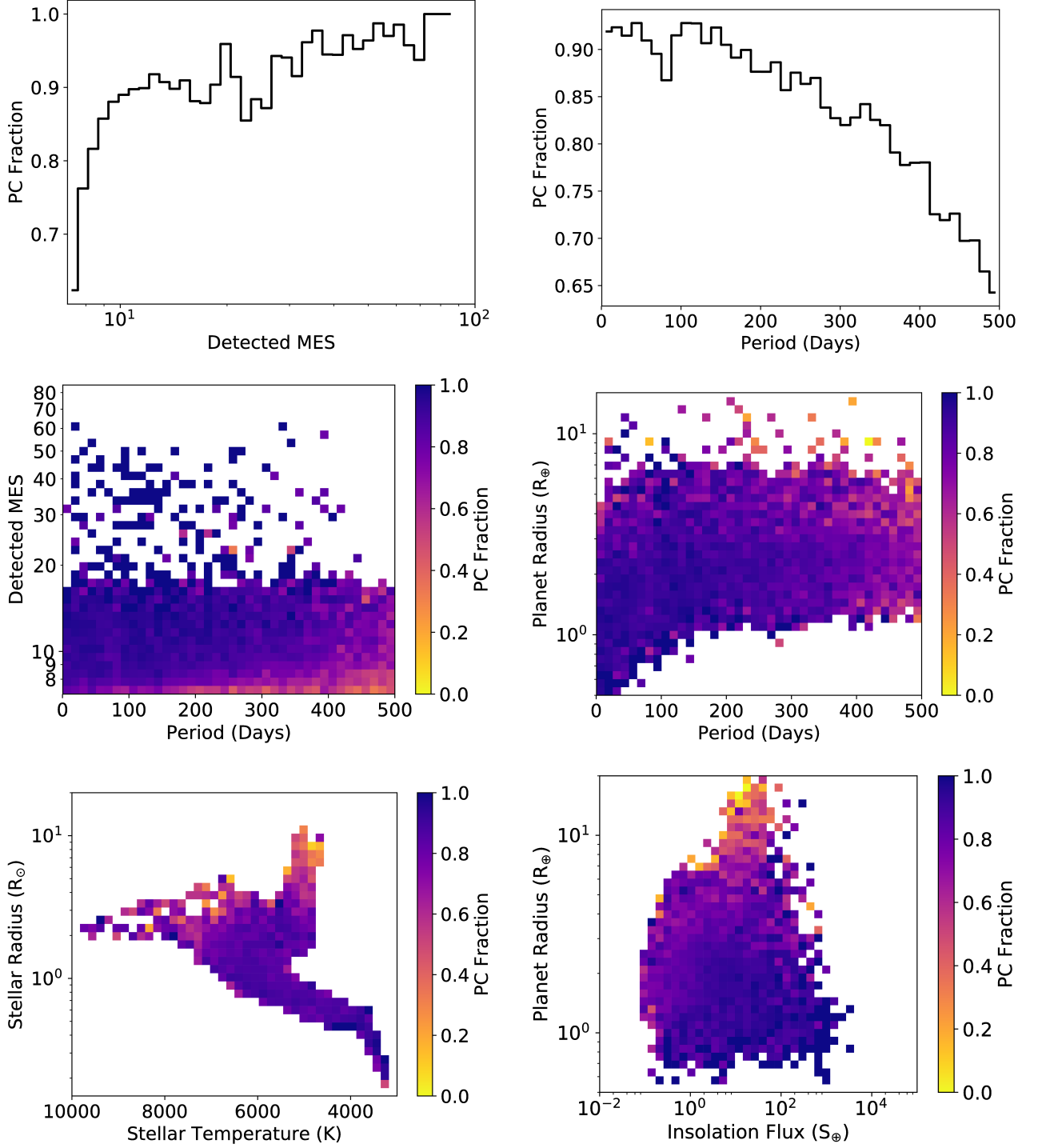
Figure 3: Examples of the PC fraction in the on-target single-injected planet population (Group 1) for different combinations of parameters. Top-left: The PC fraction as a function of the detected MES. Top-right: The PC fraction as a function of period. Middle-left: The PC fraction as a function of period and MES. Middle-right: The PC fraction as a function of period and the planet's radius. Bottom-left: The PC fraction as a function of the stellar radius and temperature. Bottom-right: The PC fraction as a function of the planet's radius and insolation flux. Note that bins/boxes with less than 5 TCEs are not displayed.

In Figure 4 we re-plot the PC fraction of the on-target injected planets as a function of period, as well as similar plots of the NTL=0, SS=0, and CO=0 fractions. This illustrates that the dip seen in the PC fraction just before $\sim$90 days is due specifically to the SS flag. The odd/even tests (designed to identify EBs detected by the *Kepler* pipeline at half their true period) only operate on TCEs with $P < 90$ days, and fail a few percent of injected planets as $P \to 90$ days. The cutoff of 90 days was chosen because natural quarter-to-quarter depth differences (a result of varying crowding values due to changing photometric apertures and stellar flux distributions) induce apparent odd/even depth differences even in true transiting planets when there is one, or less, transits per quarter (i.e., $P > 90$ days).
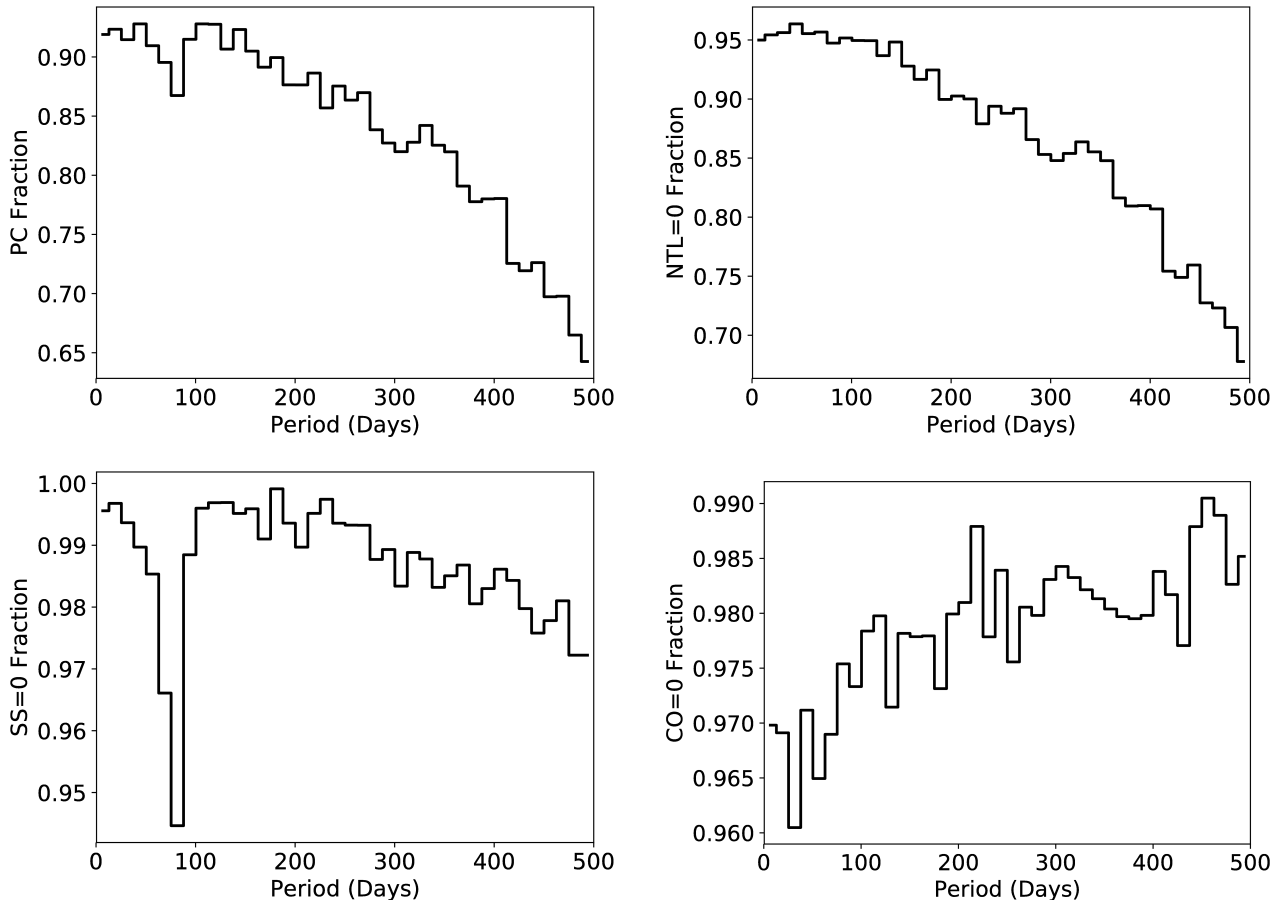

Figure 4: Examples of the PC (top-left), NTL=0 (top-right), SS=0 (bottom-left), and CO=0 (bottom-right) fractions in the on-target single-injected planet population (Group 1) as a function of period. Note that bins/boxes with less than 5 TCEs are not displayed.

In Figure 5 we show the CO=0 fraction of the 18,897 injTCEs that comprise the off-target single injected planet group (Group #2 of the injections). If the Robovetter and the Kepler Input Catalog (KIC) were perfect (see Bryson & Morton, 2017, for the types of errors that exist in the KIC), then all of these off-target planet injTCEs would be dispositioned as CO=1 (i.e., the centroid offset would be detected). In practice, only $\sim$45% of the off-target planet injections are dispositioned as CO=1, but it is worth noting that they were intentionally

injected very close to the targets ($\lesssim 1$ pixel), where it is most difficult to detect a centroid offset. When the offset distance is near 0.0 the position of the signal's origin and the position of the target become indistinguishable and the CO=0 fraction is near 100%. Also, when the MES is very low, there is not enough signal-to-noise to determine the signal location and the CO=0 fraction is near 100%. However, at large MES values and higher offset values, the CO=0 fraction tends towards zero as expected.
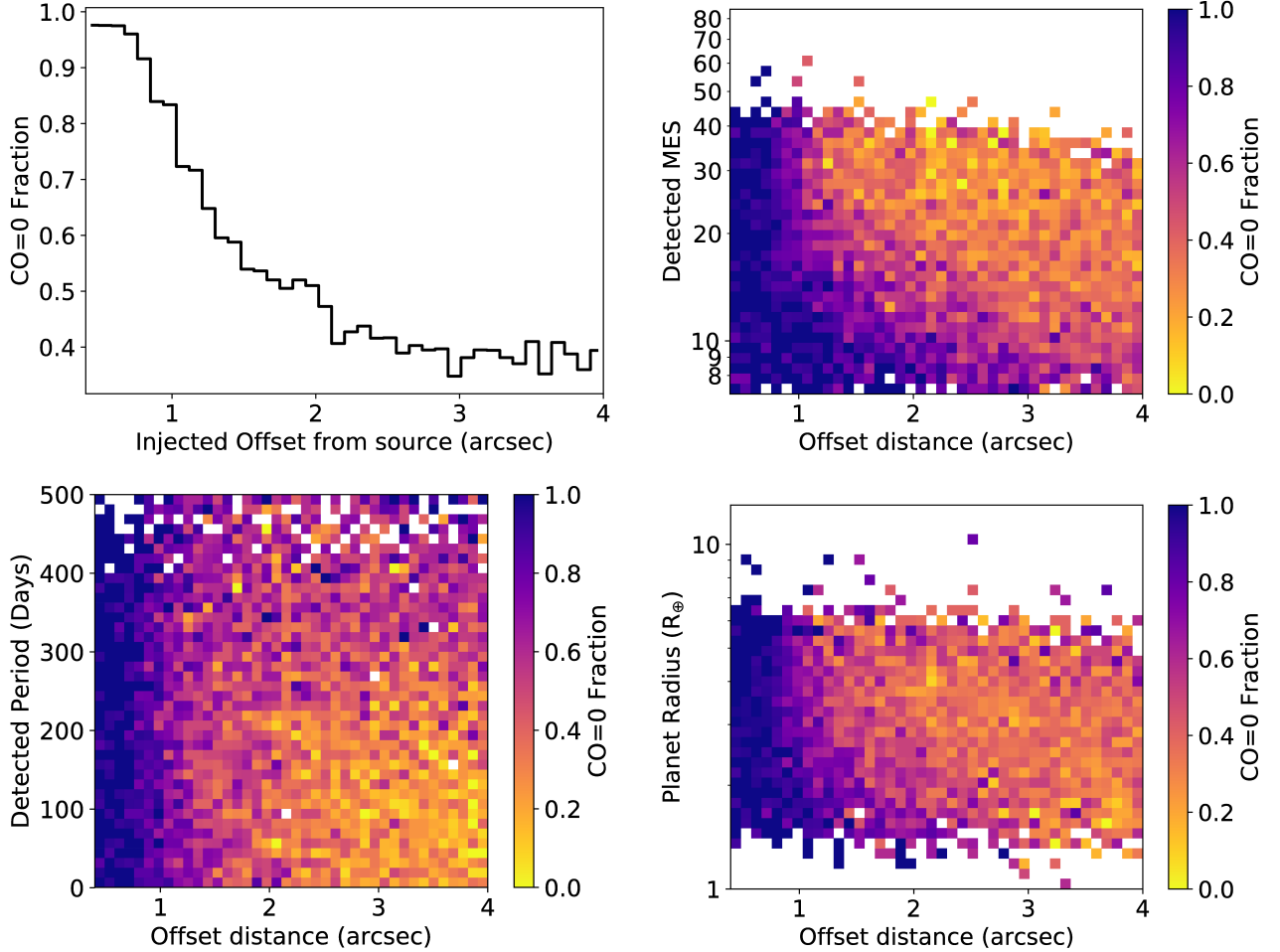

Figure 5: Examples of the CO=0 fraction in the off-target single-injected planet population (Group 2) for different combinations of parameters. Top-left: The CO=0 fraction as a function of the injected offset distance. Top-right: The CO=0 fraction as a function of the injected offset distance and MES. Bottom-left: The CO=0 fraction as a function of the injected offset distance and detected period. Bottom-right: The CO=0 fraction as a function of the injected offset distance and measured planet radius. Note that bins/boxes with less than 5 TCEs are not displayed.

In Figure 6 we show the SS=0 fraction of the 5,625 injTCEs that comprise the eclipsing binary group (Group #3 of the injections) that were detected at their injected period. If the Robovetter was perfect, all of these EB injTCEs would be dispositioned as SS=1 (i.e., the secondary would be detected). In practice, only ∼53% of the EB injections that were

recovered at their injected period are dispositioned as SS=1, but it is worth noting that half of their secondary eclipses were injected at low MES (between 0 and 10), where it is most difficult to detect a secondary eclipse. When the secondary has a very low MES (SNR) value it is often not detected, and the SS=0 fraction is near 100%. However, at large MES values, the SS=0 fraction is near 0%. While secondaries in long-period systems appear to be moderately harder to detect than in short-period systems, there does not appear to be a strong dependence on the location of the secondary in phase space or the relative duration of the secondary compared to the primary.
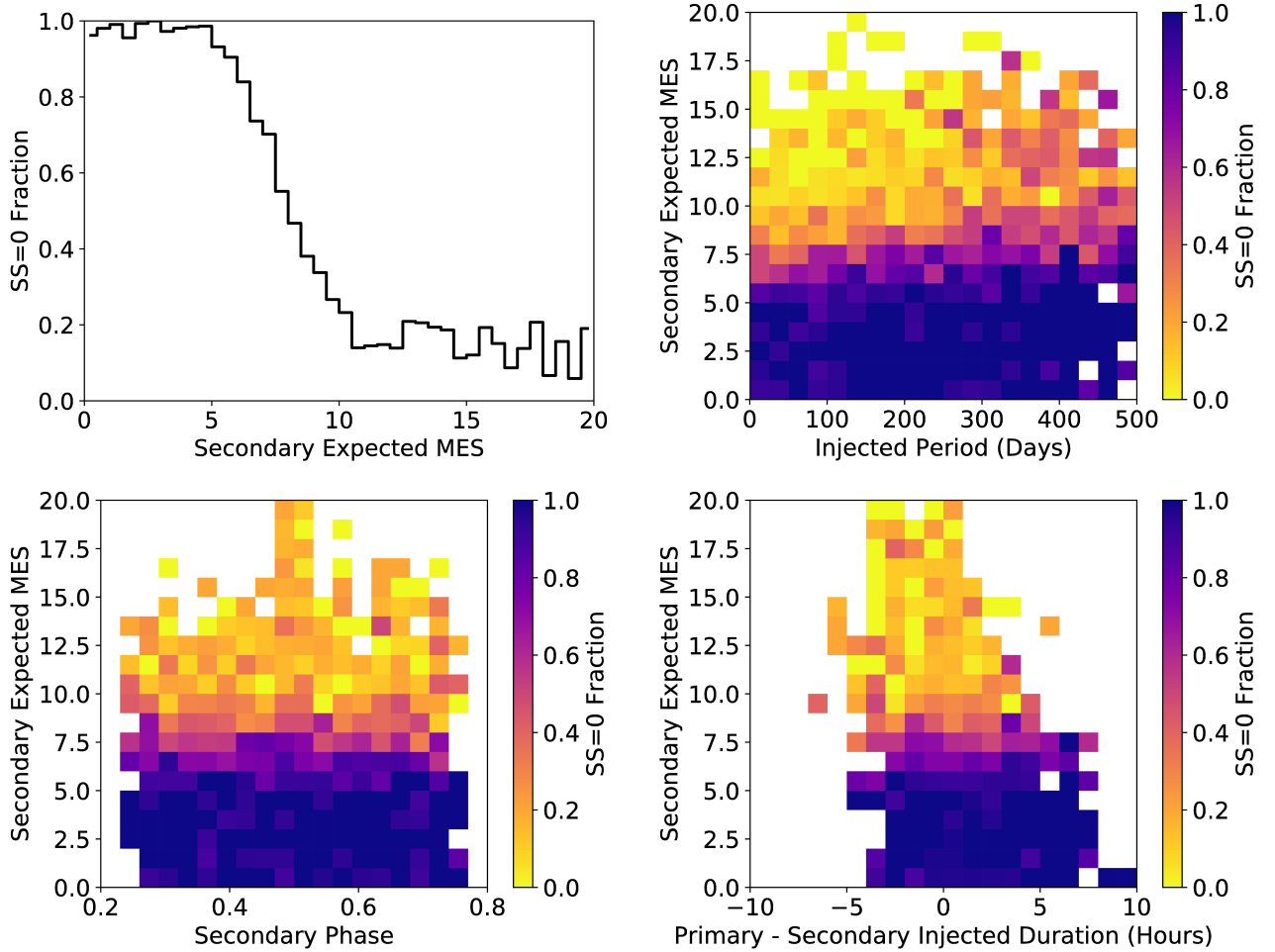

Figure 6: Examples of the SS=0 fraction in the EB injTCE population, detected by *Kepler* pipeline at their injected period, for different combinations of parameters. Top-left: The SS=0 fraction as a function of the expected MES of the secondary eclipse. Top-right: The SS=0 fraction as a function of the injected period and expected MES of the secondary eclipse. Bottom-left: The SS=0 fraction as a function of the phase of the secondary and the expected MES of the secondary eclipse. Bottom-right: The SS=0 fraction as a function of the difference in duration of the primary and secondary eclipses, and the expected MES of the secondary eclipse. Note that bins/boxes with less than 5 TCEs are not displayed.

In Figure 7 we show the SS=0 fraction of the 5,625 injTCEs that comprise the eclipsing binary group (Group #3 of the injections) that were detected at half their injected period (commonly referred to as "odd/even EBs"). If the Robovetter was perfect, all of these EB injTCEs would be dispositioned as SS=1 (i.e., the secondary would be detected due to differences between the odd- and even-numbered eclipses). In practice, only ~16% of EB injections that were recovered at half their injected period are dispositioned as SS=1. However, it is worth noting that in most of these cases the secondary was injected with very similar depth and duration as the primary, and very near phase 0.5, which is the region of parameter space where it is most difficult to detect a secondary. In other words, when the difference in MES between the primary and secondary eclipses is near 0.0, and the secondary is very near phase 0.5 with a duration that matches the primary, then the odd/even effect is not detectable and the SS=0 fraction is near 100%. The SS=0 fraction decreases as the difference in MES between the primary and secondary eclipses increases, the secondary eclipse's phase deviates from 0.5, or the durations of the primary and secondary eclipses diverge. Note that the empty areas in the histograms are regions of parameter space where the *Kepler* pipeline itself detected the odd/even effect before making a TCE, and thus created the TCE at the correct orbital period. Also note that the Robovetter odd/even tests are not applied to TCEs with detected periods greater than 90 days (or an injected period greater than 180 days), due to depth differences that naturally occur on a quarterly basis as a result of CCD response, aperture, and crowding differences.

In Figure 8 we show the PC fraction of the 19,536 invTCEs. We have removed all targets that are associated with KOIs, as well as some known lensing candidates, so that this "cleaned" set better represents the types of false positives found in the observed set. If the Robovetter was perfect, all of these "cleaned" invTCEs would be dispositioned as FP. In practice, ~99.5% of them are dispositioned as FP. The few invTCEs dispositioned as PC occur at low MES. Note that, given the small number statistics, caution is encouraged when interpreting these plots.

In Figure 9 we show the PC fraction of the 19,536 scrTCEs. We have removed all targets that are associated with KOIs to create a "cleaned" set that better represents the types of false positives found in the observed set. If the Robovetter was perfect, all of these "cleaned" scrTCEs would be dispositioned as FP. In practice, ~99.7% of them are dispositioned as FP. The few scrTCEs dispositioned as PC occur at low MES. Note that, given the small number statistics, caution is encouraged when interpreting these plots.

Finally, as an example for those interested in using this information for occurrence rate calculations, we look at the PC rate of injTCEs with radius (R_p) and insolation flux (S_p) values within 25% of that of Earth's values (i.e., $0.75 > R_p > 1.25\ R_\oplus$ and $0.75 > S_p > 1.25\ S_\oplus$). There are 224 injTCEs that meet these R_p and S_p criteria, of which 200 are designated planet candidates by the Robovetter, therefore yielding a completeness of 89.3%. In the same parameter space, using the "cleaned" sets, there are 34 invTCEs and 41 scrTCEs, for a total of 75, of which 1 passes as PC, for an effectiveness of 98.7%. The reader is encouraged to use the Robovetter Disposition Tables (§3) to perform analyses similar to those presented here for any sample of *Kepler* targets used for occurrence rate studies and incorporate the inferred corrections into their calculations.
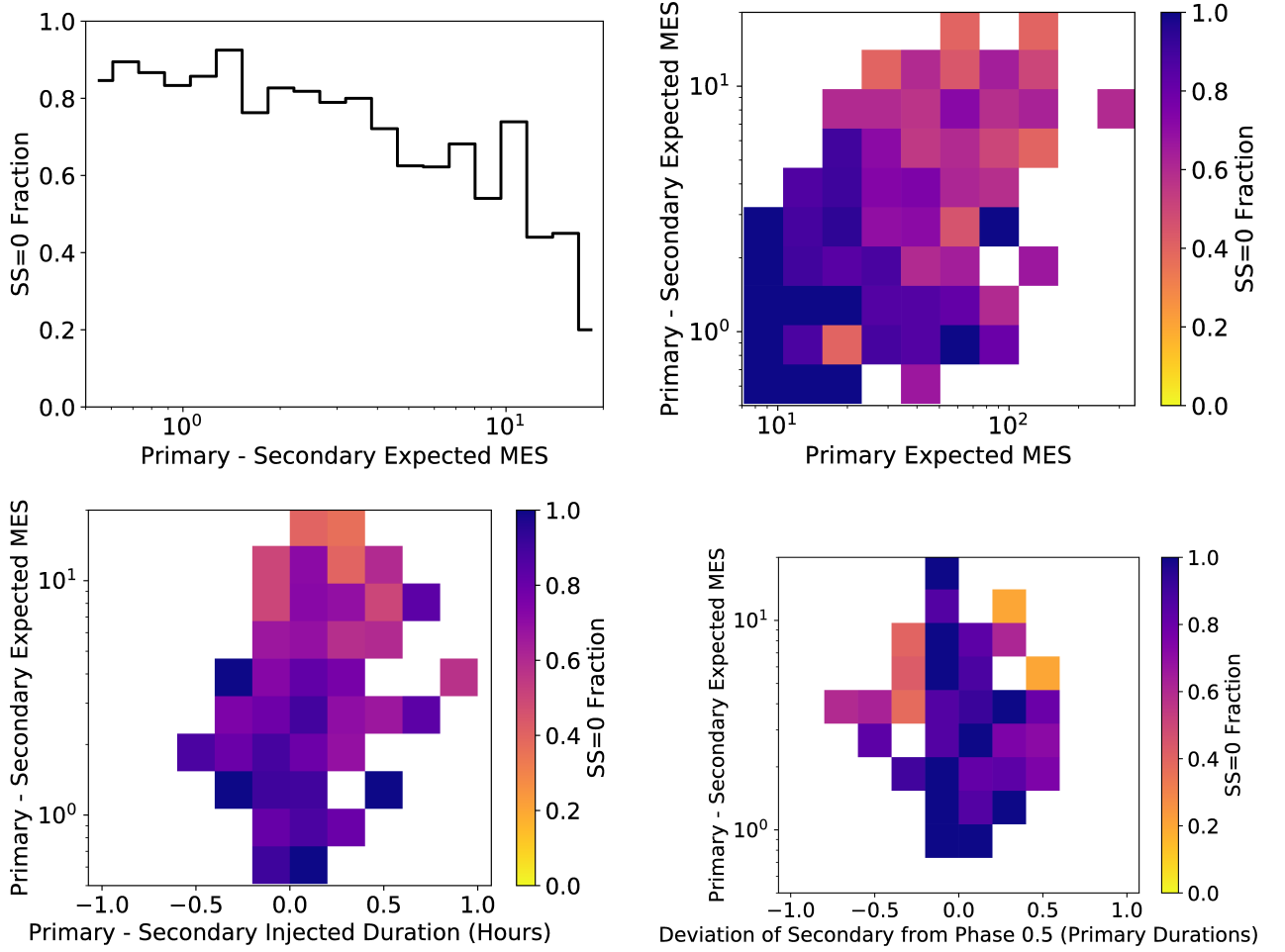
Figure 7: Examples of the SS=0 fraction in the EB injTCE population, detected by the *Kepler* pipeline at half their injected period, for injected periods less than 180 days and different combinations of parameters. Top-left: The SS=0 fraction as a function of the difference between the expected MES of the primary and secondary eclipses. Top-right: The SS=0 fraction as a function of the expected MES of the primary eclipse and the difference between the expected MES of the primary and secondary eclipses. Bottom-left: The SS=0 fraction as a function of the difference in duration of the primary and secondary eclipses and the difference between the expected MES of the primary and secondary eclipses. Bottom-right: The SS=0 fraction as a function of the deviation of the phase of the secondary from 0.5 and the difference between the expected MES of the primary and secondary eclipses. Note that bins/boxes with less than 5 TCEs are not displayed.
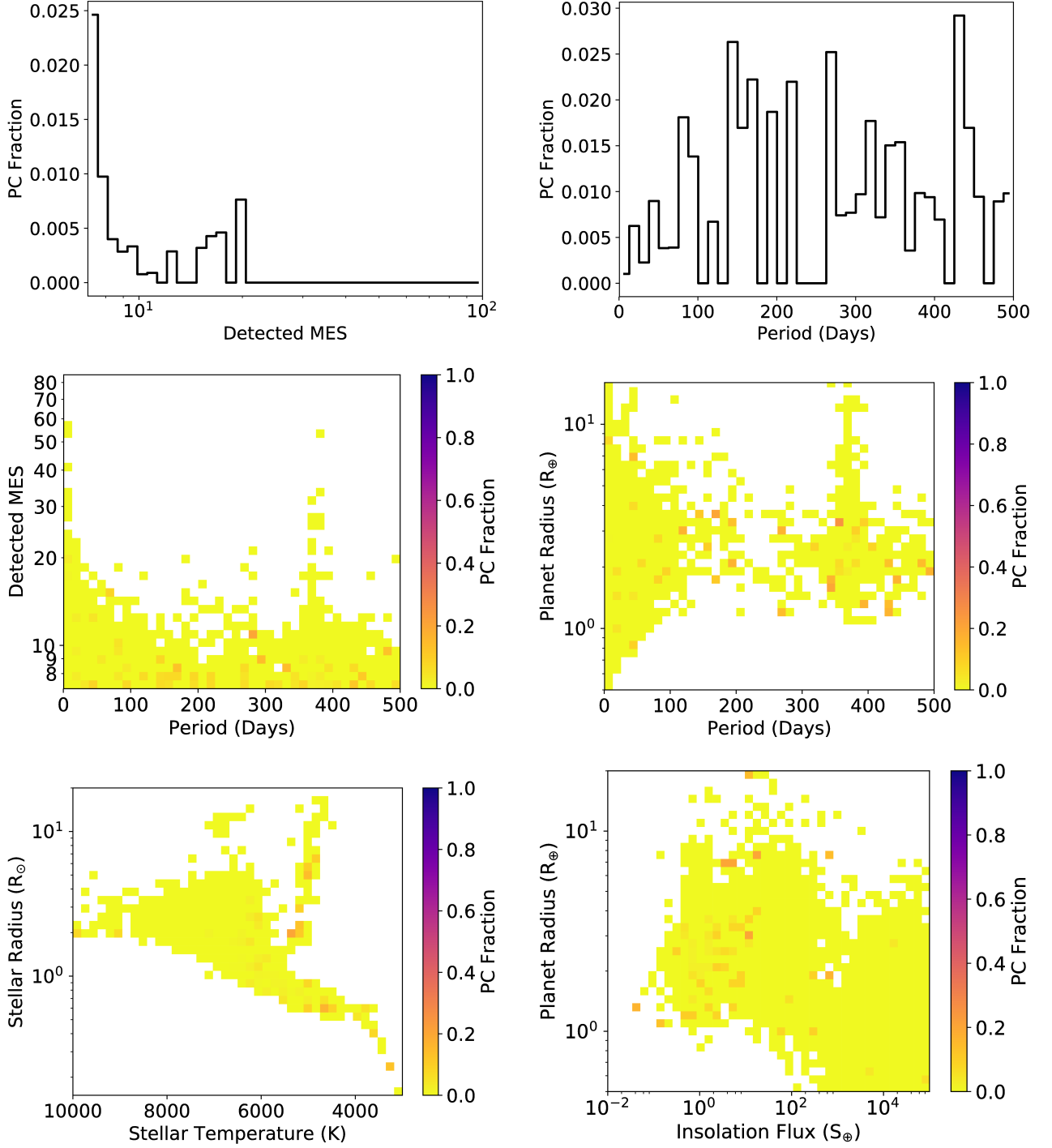
Figure 8: Examples of the PC fraction of the invTCE population for different combinations of parameters. Top-left: The PC fraction as a function of the detected MES. Top-right: The PC fraction as a function of period. Middle-left: The PC fraction as a function of period and MES. Middle-right: The PC fraction as a function of period and the planet's radius. Bottom-left: The PC fraction as a function of the stellar radius and temperature. Bottom-right: The PC fraction as a function of the planet's radius and insolation flux. Note that bins/boxes with less than 5 TCEs are not displayed.
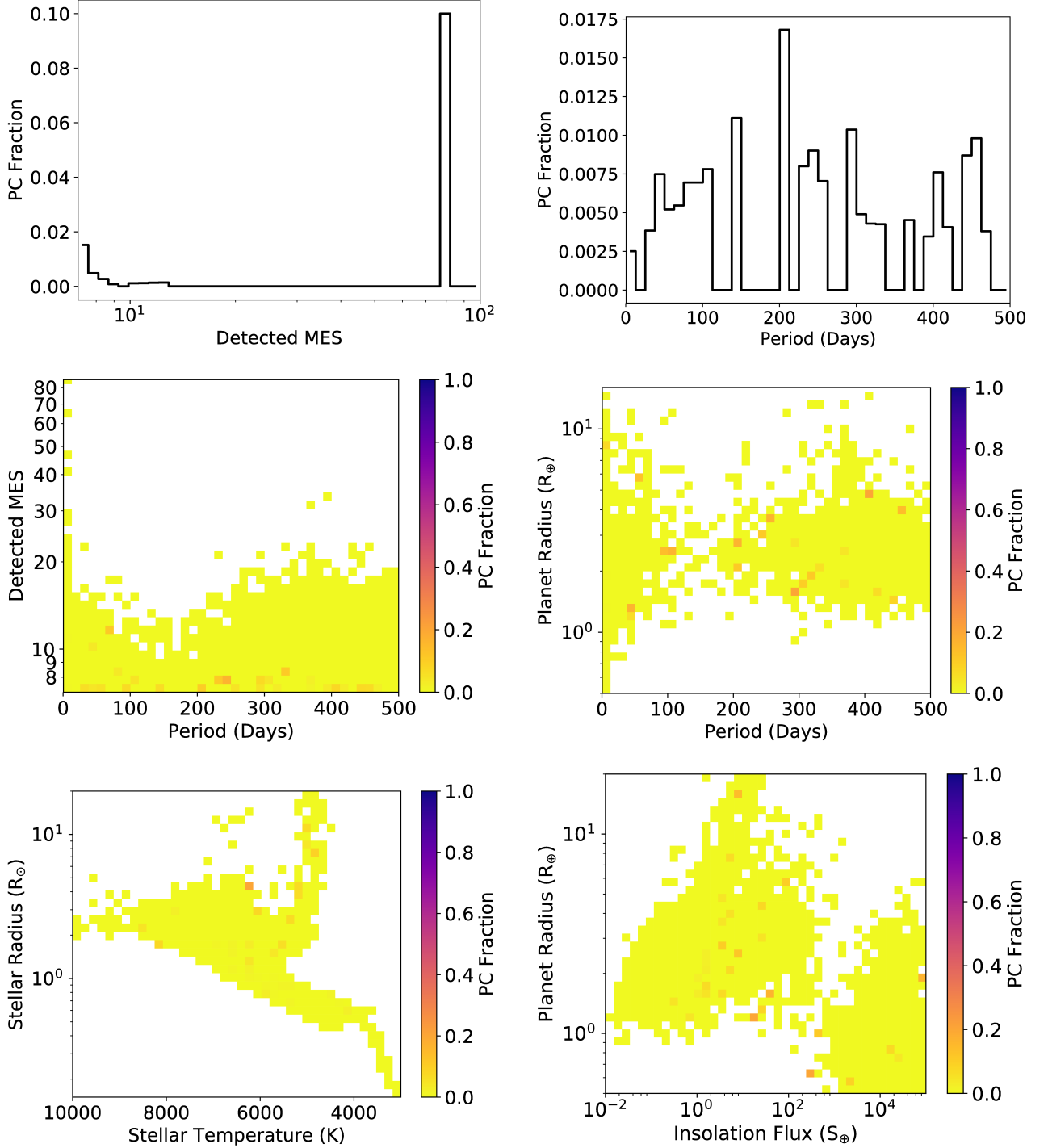
Figure 9: Examples of the PC fraction of the scrTCE (set #1) population for different combinations of parameters. Top-left: The PC fraction as a function of the detected MES. Top-right: The PC fraction as a function of period. Middle-left: The PC fraction as a function of period and MES. Middle-right: The PC fraction as a function of period and the planet's radius. Bottom-left: The PC fraction as a function of the stellar radius and temperature. Bottom-right: The PC fraction as a function of the planet's radius and insolation flux. Note that bins/boxes with less than 5 TCEs are not displayed.

References

Batalha, N. M., Rowe, J. F., Bryson, S. T., et al. 2013, ApJS, 204, 24

Borucki, W. J., Koch, D. G., Basri, G., et al. 2011a, ApJ, 728, 117

—. 2011b, ApJ, 736, 19

Bryson, S. T., & Morton, T. D. 2017, Planet Reliability Metrics: Astrophysical Positional Probabilities for Data Release 25 (KSCI-19108-001)

Burke, C. J., & Catanzarite, J. 2017a, Planet Detection Metrics: Completeness Contour Model for Data Release 25 (KSCI-19111-001)

—. 2017b, Planet Detection Metrics: Per-Target Flux-Level Transit Injection Tests of TPS for Data Release 25 (KSCI-19109-001)

—. 2017c, Planet Detection Metrics: Window and One-Sigma Depth Functions for Data Release 25 (KSCI-19101-002)

Burke, C. J., Bryson, S. T., Mullally, F., et al. 2014, ApJS, 210, 19

Christiansen, J. L. 2017, Planet Detection Metrics: Pixel-Level Transit Injection Tests of Pipeline Detection Efficiency for Data Release 25 (KSCI-19110-001)

Coughlin, J. L. 2017, Description of the TCERT Vetting Products for the Data Release 25 Catalog (KSCI-19105-001)

Coughlin, J. L., Mullally, F., Thompson, S. E., et al. 2016, ApJS, 224, 12

Jenkins, J. M. 2017, *Kepler* Mission Data Processing Handbook (KSCI-19081-002)

Mullally, F. 2017, Automatic Detection of Background Objects using the Centroid Robovetter (KSCI-19115-001)

Mullally, F., Coughlin, J. L., Thompson, S. E., et al. 2015a, ApJS, 217, 31

Rowe, J. F., Coughlin, J. L., Antoci, V., et al. 2015, ApJS, 217, 16

Thompson, S. E., Caldwell, D. A., Jenkins, J. M., et al. 2016, *Kepler* Data Release 25 Notes (KSCI-19065-002)

Thompson, S. E., Coughlin, J. L., Mullally, F. M., et al. 2017, ApJS, in prep.

Twicken, J. D., Jenkins, J. M., Seader, S. E., et al. 2016, AJ, 152, 158

Van Cleve, J., Christiansen, J. L., Jenkins, J. M., et al. 2016, *Kepler* Data Characterization Handbook (KSCI-19040-005)